JOURNAL OF MATERIAL SCIENCE 27 (1992) 2713–2718

Preparation of monodispersed, uniform particles of ZnO and Al_2O_3 and application for $ZnAl_2O_4$ formation

T. TSUCHIDA, S. KITAJIMA
Department of Applied Chemistry, Faculty of Engineering, Hokkaido University, Sapporo 060, Japan

Monodispersed, hexagonal prismatic and spindle-shaped zinc oxide particles and spherical hydrated alumina particles have been prepared by hydrolysing dilute solutions of sulphate and nitrate at elevated temperatures in the presence of urea. The phenomenological behaviour of $ZnAl_2O_4$ formation between such particles has been observed by scanning electron microscopy (SEM).

1. Introduction

Zinc oxide and aluminium oxide are used in a variety of ceramic applications such as varistors, semiconductors, abrasives, refractories and so on. The use of monodispersed (less than a few micrometres in size), uniform (spherical or equiaxed in shape) ceramic powders is desirable to achieve a uniform sintered microstructure. Such particles are also of much interest as model materials for theoretical studies of not only sintering, but also of solid state reactions. Because of the ease of SEM observation of the change in size and microstructure of these particles during a reaction, it can be expected to obtain useful information on the reaction mechanism from SEM.

The purpose of the present study is to prepare monodispersed, uniform particles of ZnO and Al_2O_3 by the homogeneous hydrolysis procedures, and to obtain some information on the reaction behaviours between ZnO and Al_2O_3 particles by SEM observation.

2. Experimental procedure

The preparation conditions of zinc oxides and hydrated alumina are shown in Table I. All stock solutions were prepared from guaranteed-grade $ZnSO_4 \cdot 7H_2O$, $Zn(NO_3)_2 \cdot 6H_2O$, $Al_2(SO_4)_3 \cdot 18H_2O$ and $CO(NH_2)_2$ in doubly distilled water. The solutions of zinc sulphate, zinc nitrate or aluminium sulphate (1 l) and urea (1 l) were kept in a flask (2 l) and heated up to 95 °C in the former two cases and to 90 °C in the latter one at a rate of 0.5 °C min^{-1}. The former solutions became turbid at around 90 °C and the latter one at around 80 °C. After an ageing period of 2 h, the solutions were rapidly quenched to room temperature. Subsequently, the precipitates were separated on a microfilter (0.22 μm pore size), washed with four 20 ml portions doubly distilled water, dried at 110 °C for 12 h and kept in a desiccator. The precipitated zinc oxides, ZnO(S) and ZnO(N) which were prepared from zinc sulphate and nitrate, contained a small amount of basic zinc carbonate, $4ZnO \cdot CO_2 \cdot 4H_2O$ [1] and were then calcined, to obtain a single phase of ZnO(S) and ZnO(N), at 300 °C for 30 min. Precipitated hydrated alumina was amorphous to X-ray [2] and was then calcined, to form η-Al_2O_3, at 900 °C for 30 min. The equimolar mixture of ZnO(S) or ZnO(N) (2×10^{-5} mol) and η-Al_2O_3 (2×10^{-5} mol) was prepared by wet mixing in ethanol. This wet mixture was placed on a platinum plate (3 mm × 5 mm), dried and then heated to given temperatures (700–1300 °C) at a rate of 10 °C min^{-1} using a themogravimetric–differ-

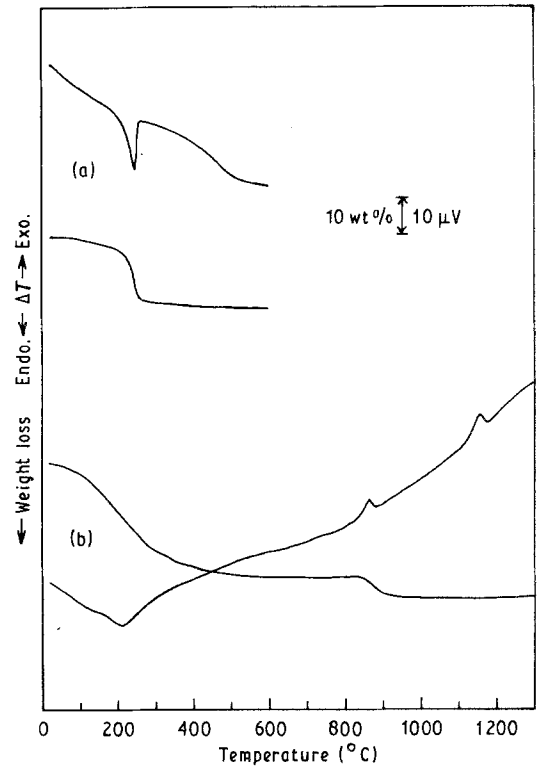

Figure 1 TG and DTA curves of precipitated: (a) ZnO(S) and (b) hydrated alumina.

0022–2461

TABLE I Preparation conditions of zinc oxides and hydrated alumina

Solution composition	Ageing temperature (°C)	Ageing time (h)
2×10^{-3} mol l^{-1} $ZnSO_4 \cdot 7H_2O + 8 \times 10^{-2}$ mol l^{-1} $CO(NH_2)_2$	95	2
1×10^{-3} mol l^{-1} $Zn(NO_3)_3 \cdot 6H_2O + 1 \times 10^{-1}$ mol l^{-1} $CO(NH_2)_2$	95	2
1×10^{-3} mol l^{-1} $Al_2(SO_4)_3 \cdot 18H_2O + 1.5 \times 10^{-1}$ mol l^{-1} $CO(NH_2)_2$	90	2

ential thermal analysis (TG–DTA) apparatus (Rigaku Denki Co. Model 8085). The plate was fixed on a quartz glass plate with a double-sided cellulose tape and subjected to X-ray diffraction (XRD). Subsequently, the plate was placed on the brass stubs, coated with a sputtering-deposited gold film of about 20 nm in thickness and subjected to SEM and energy dispersive X-ray spectroscopy (EDX). For the sake of comparison, zinc oxide particles alone were also heated and subjected to SEM.

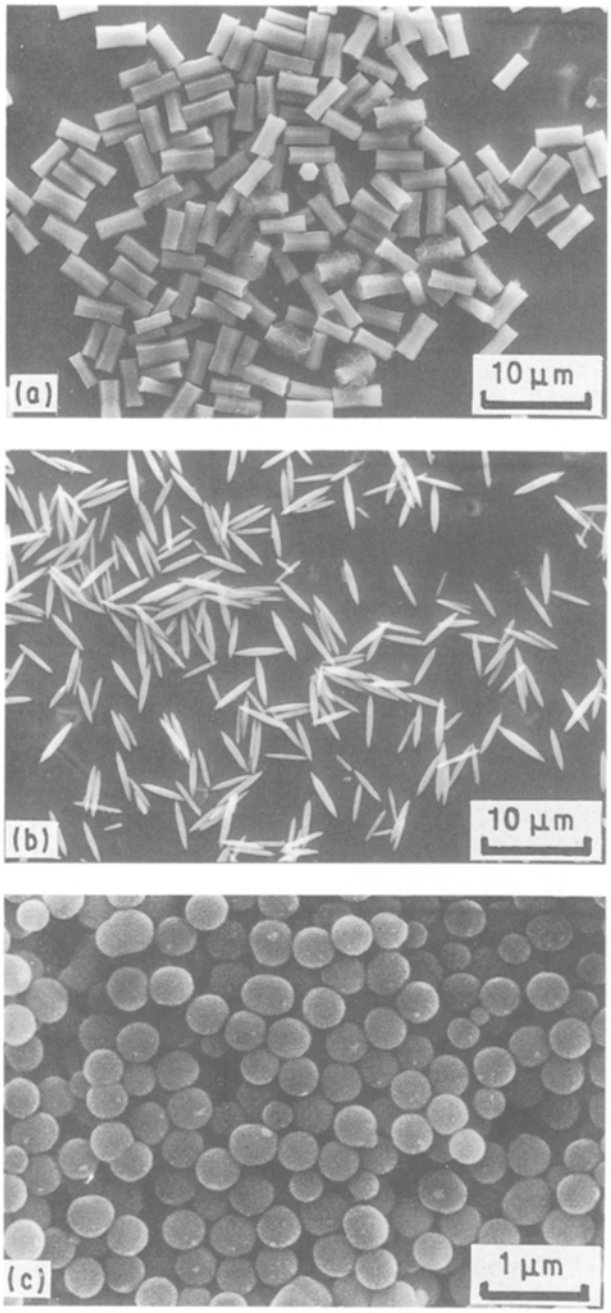

Figure 2 Scanning electron micrographs of precipitated: (a) ZnO(S); (b) ZnO(N) and (c) hydrated alumina.

3. Results and discussion

Fig. 1 shows TG–DTA curves of precipitated ZnO(S) and hydrated alumina. An endothermic peak for ZnO(S) at 250 °C was attributable to the thermal decomposition of $4ZnO \cdot CO_2 \cdot 4H_2O$ coexisted with zinc oxides. The weight loss was 19.3 wt %. The TG–DTA curves of precipitated ZnO(N), though not shown in the figure, were very similar to those of ZnO(S), except for the weight loss of 16.5 wt %. On the other hand, the DTA curve of hydrated alumina shows a broad endothermic peak at 210 °C and two exothermic peaks at 862 and 1145 °C. The former peak is due to the dehydration of amorphous hydrated alumina to amorphous alumina [2] having a weight loss of 36.7 wt % in TG, which may be comparable to the theoretical weight loss of aluminium trihydroxide, $Al_2O_3 \cdot 3H_2O$(i.e., 34.6 wt %). The exothermic peak at 862 °C is due to the crystallization of the amorphous alumina to η-Al_2O_3, and the second peak is due to the transformation of η-Al_2O_3 to α-Al_2O_3 [2]. The weight loss at around 850 °C is due to the desulphurization of sulphate ions which remained in the amorphous hydrated alumina. This sulphate ion was also

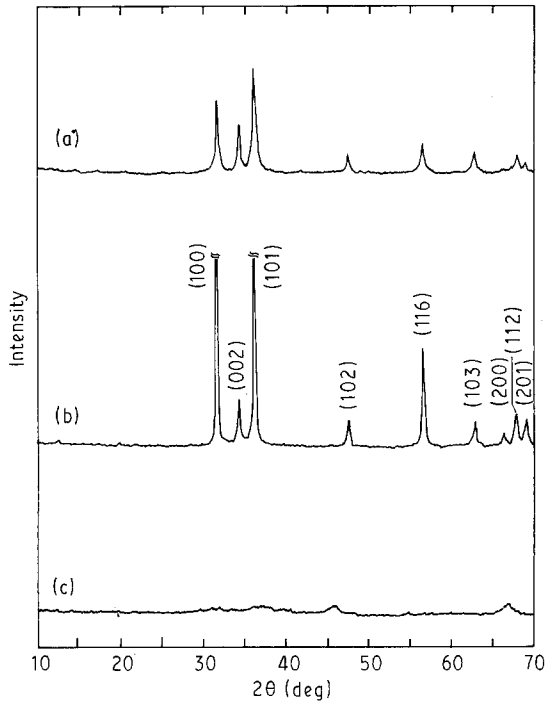

Figure 3 X-ray diffraction patterns of: (a) ZnO(S) and (b) ZnO(N) obtained by calcining precipitated zinc oxides at 300 °C for 30 min, and (c) η-Al_2O_3 obtained by calcining hydrated alumina at 900 °C for 30 min.

easily removed by washing with a dilute ammonium hydroxide [2].

Fig. 2 shows scanning electron micrographs of precipitated ZnO(S), ZnO(N) and amorphous hydrated alumina. The particles of ZnO(S) and ZnO(N) show the monodispersed, hexagonal prismatic (1.9 μm width, 4.3 μm length) and spindle-shaped (0.8 μm in width, 5 μm length) morphology. The particle size and morphology of zinc oxides depended on the concentration of stock solutions and ageing time. With increasing concentration of zinc sulphate solution, the zinc oxide particles became wide and short, and with increasing concentration of urea and ageing time, the amount of $4ZnO \cdot CO_2 \cdot 4H_2O$ increased. On the other hand, hydrated alumina shows the monodispersed, spherical particles of 0.5–0.6 μm in size. Although the particle size tended to increase with increasing concentration of aluminium sulphate, the best monosized particles were obtained at the concentration shown in Table I. When the precipitated zinc oxides were calcined at 300 °C for 30 min and hydrated alumina at 900 °C for 30 min, the shape and size of these particles remained almost unchanged, except for a slight decrease in size of hydrated alumina ($\sim$ 0.1 μm).

Fig. 3 shows the X-ray diffraction patterns of the calcined ZnO(S), ZnO(N) and η-Al_2O_3. Comparing the XRD patterns of ZnO(S) with ZnO(N), the intensity ratio I_{002}/I_{100} or I_{002}/I_{101} remarkably decreased in the latter. The magnitude of this intensity ratio for the ZnO(S) and ZnO(N) samples hardly changed, even when, in order to avoid a preferential orientation of particles, the samples were mixed with a pasty starch, dried and then subjected to XRD. Therefore, the fact that the intensity ratio is smaller in the ZnO(N) sample reflects the spindle-shaped morphology which does not contain the hexagonal basal plane

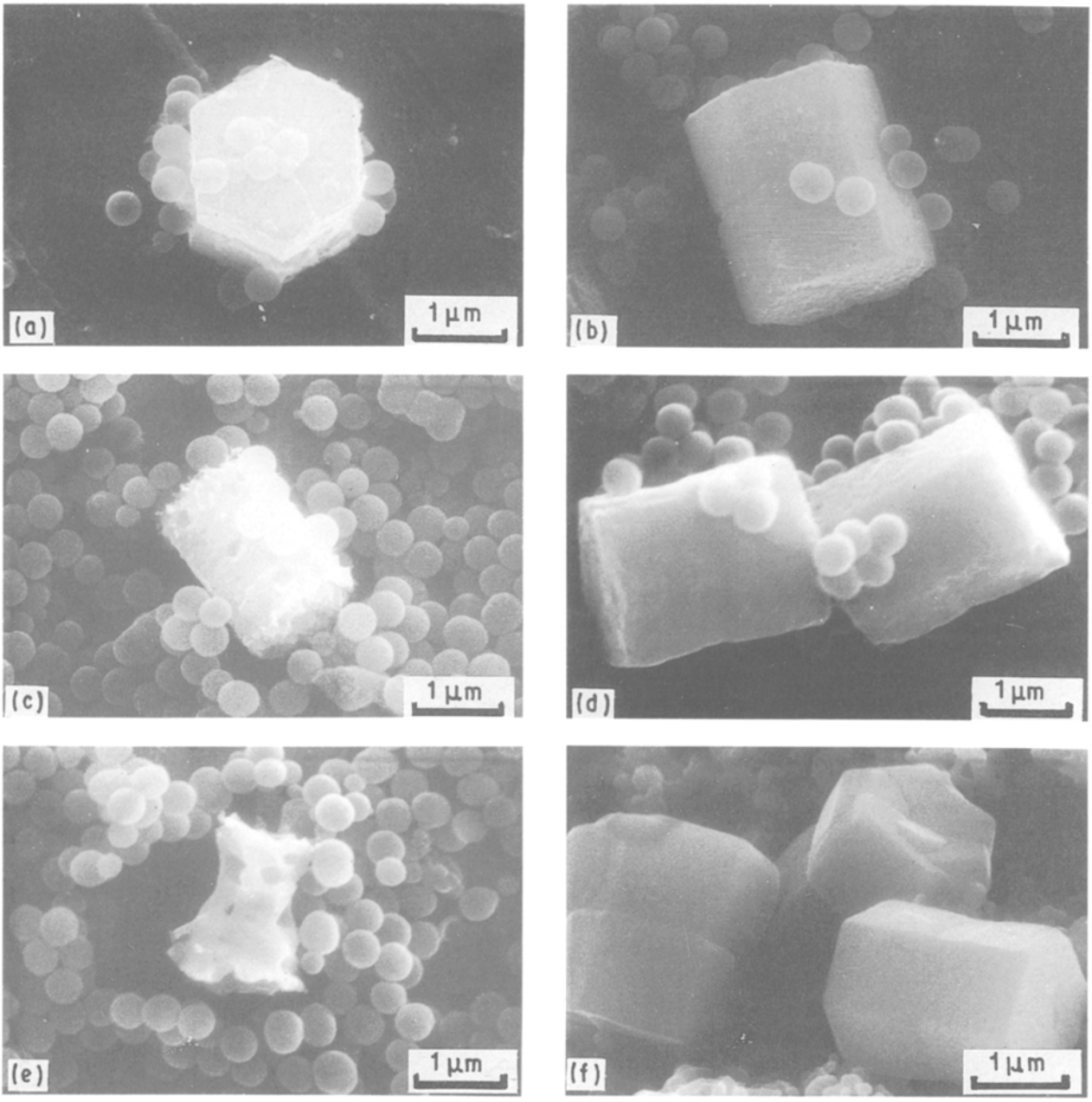

Figure 4 Scanning electron micrographs for ZnO(S)–η-Al_2O_3 mixture: (a) before the reaction, and heated in TG–DTA apparatus; (b) 800 °C for 0 h; (c) 800 °C for 2 h; (d) 1000 °C for 0 h; (e) 1000 °C for 2 h, and (f) ZnO(S) heated alone at 1000 °C for 2 h.

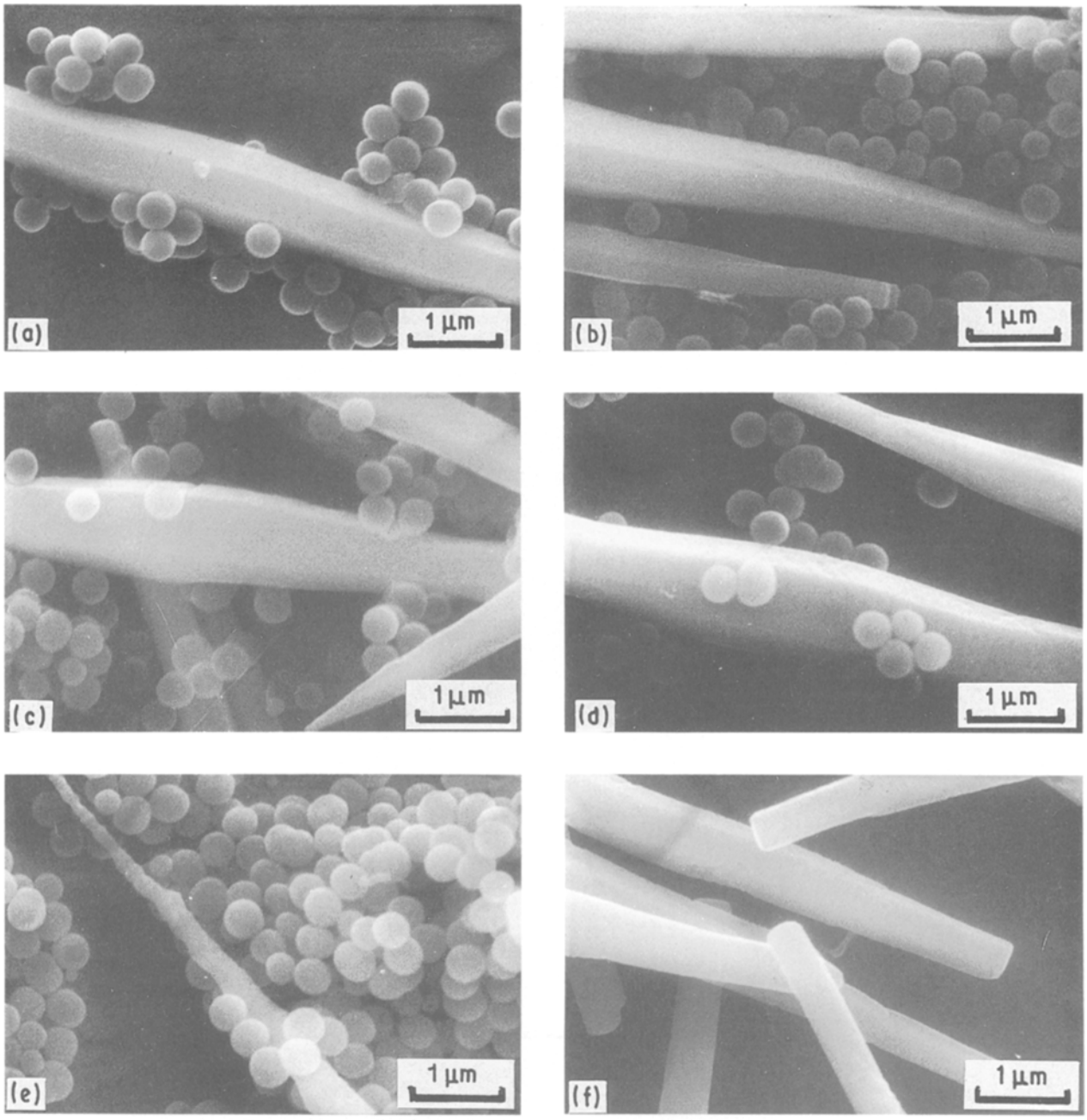

Figure 5 Scanning electron micrographs for ZnO(N)–η-Al_2O_3 mixture: (a) before the reaction, and heated in TG–DTA apparatus; (b) 800 °C for 0 h; (c) 800 °C for 2 h; (d) 1000 °C for 0 h; (e) 1000 °C for 2 h, and (f) ZnO(N) heated alone at 1000 °C for 2 h.

shown in ZnO(S). The XRD patterns in Fig. 3c show a poorly-crystallized η-Al_2O_3.

Figs 4 and 5 show scanning electron micrographs of ZnO(S)–η-Al_2O_3 and ZnO(N)–η-Al_2O_3 mixtures before and after the reaction. From Figs 4a and 5a, it can be seen that the real contact condition between ZnO and η-Al_2O_3 particles before the reaction is discontinuous and incomplete. On heating the ZnO(S)–η-Al_2O_3 mixture to 800 °C (Fig. 4b), the unevenness of the hexagonal basal plane of ZnO(S) particle can be observed. With increasing temperature and time, the unevenness became remarkable over the whole surface of ZnO(S) particle and then the particle size became much smaller, as shown in Fig. 4e. On the contrary, the shape and size of η-Al_2O_3 remained unchanged. In the case of the ZnO(N)–η-Al_2O_3 mixture, the head of the spindle-shaped ZnO(N) particle became sharper on heating at 800 °C for 2 h (Fig. 5c). Further heating at 1000 °C for 2 h (Fig. 5e) resulted in very fine ZnO(N) particles. On the other hand, as can be seen from Figs 4f and 5f, even when ZnO(S) and ZnO(N) particles are heated alone at 1000 °C for 2 h, no change in the surface of ZnO could be observed. Therefore, the changes in shape and size of ZnO(S) and ZnO(N) particles observed when the mixtures were heated at 800 °C are probably correlated to the formation of $ZnAl_2O_4$. The $ZnAl_2O_4$ product was barely detected by XRD when heated at 1000 °C for 30 min, because of a very small amount of reaction mixture and a low-crystallized product.

Fig. 6 shows scanning electron micrograph of the ZnO(N)–η-Al_2O_3 mixture reacted at 1000° for 2 h and

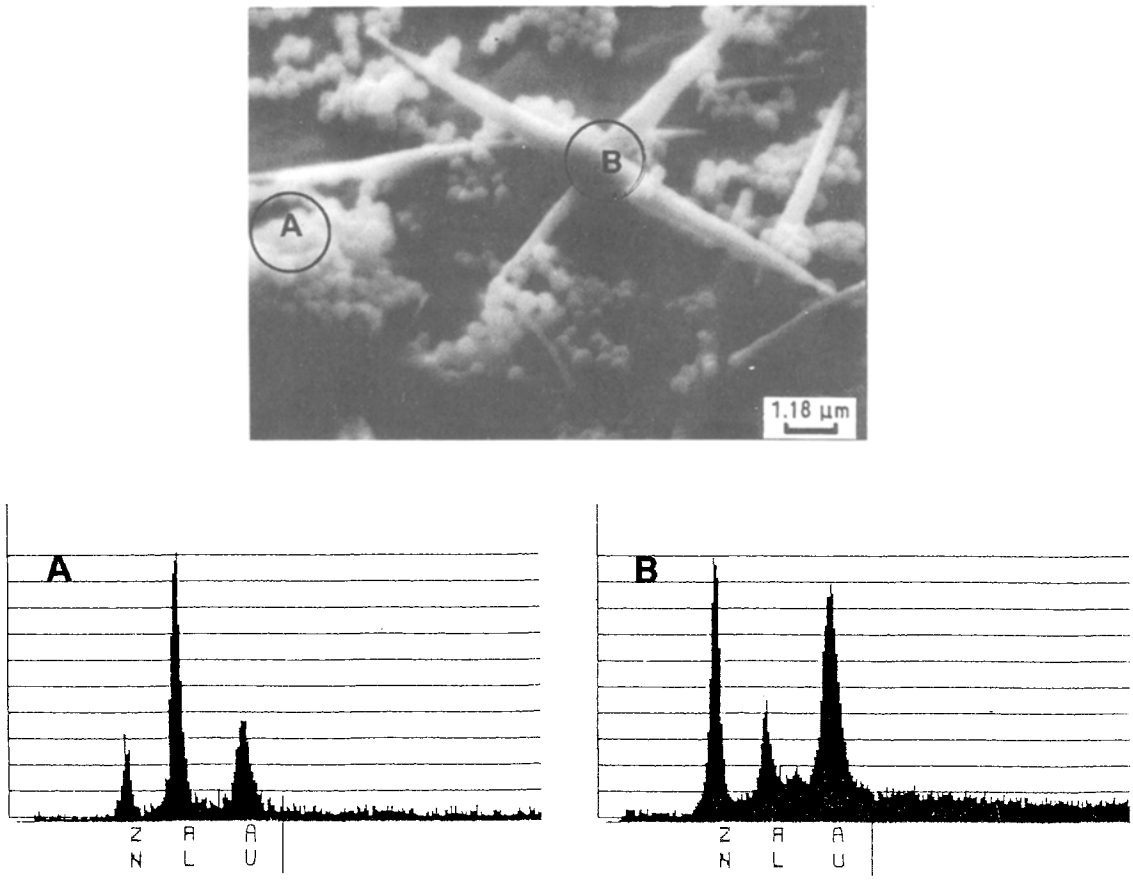

Figure 6 Scanning electron micrograph for ZnO(N)–η-Al_2O_3 mixture reacted at 1000 °C for 2 h, and EDX profiles taken from spot A on η-Al_2O_3 particles and spot B on ZnO(N) particles.

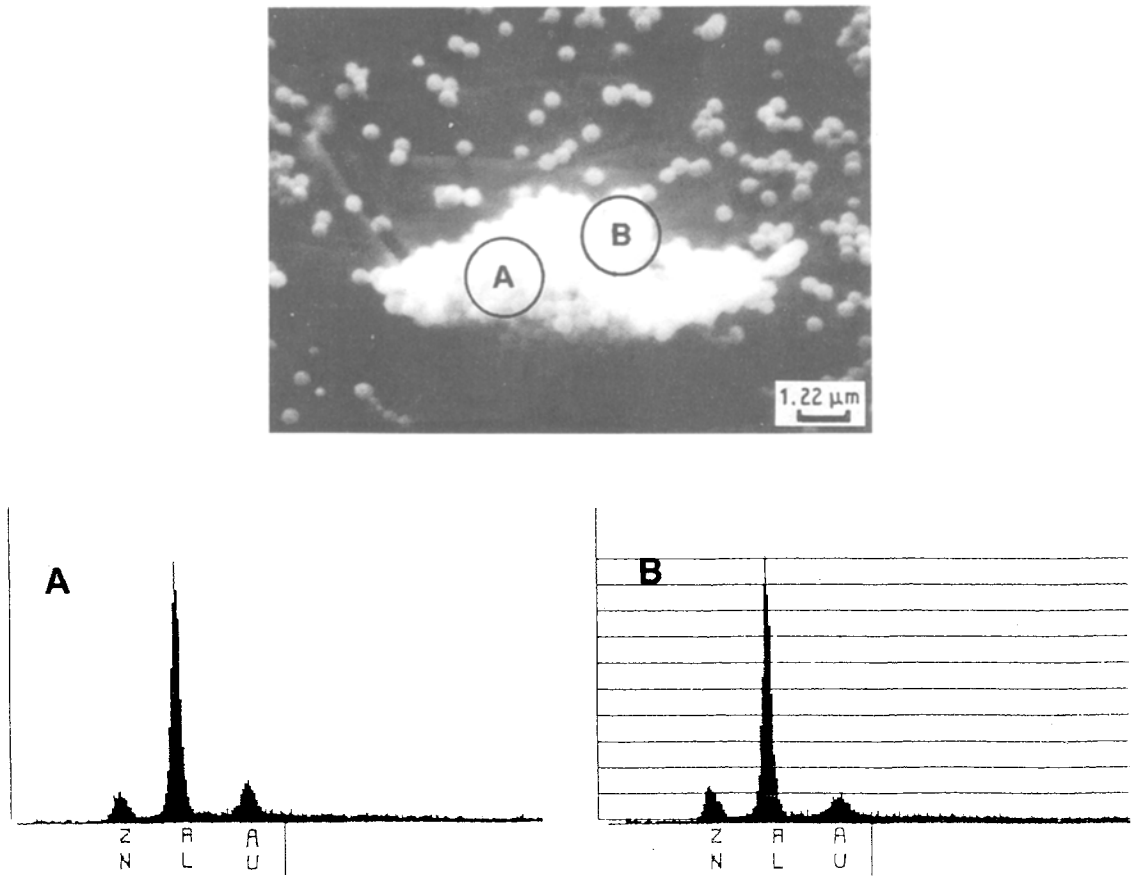

Figure 7 Scanning electron micrograph for spherical η-Al_2O_3 particles obtained after removal of unreacted ZnO particles from the mixture shown in Fig. 6 by dissolution with a NH_4Cl–NH_4OH solution, and EDX profiles taken from spots A and B.

EDX profiles taken from the spot A on η-Al_2O_3 particles and the spot B on ZnO(N) particles. The ZnK_α and AlK_α profiles were detected on both spots A and B, though different in intensity. This seems to indicate the formation of $ZnAl_2O_4$ phase on both particles. However, the diameter of the electron beam used was 2 μm which was much larger than the diameter of η-Al_2O_3 (0.5 μm) and the width of ZnO(N) (0.8 μm) so that the ZnK_α and AlK_α profiles were reflected from both particles of ZnO and η-Al_2O_3. This problem was improved when larger ZnO particles (10–20 μm in size) were used for the reaction, and the AlK_α profile was not detected on the surface of the ZnO particle [2]. Moreover, after the dissolution of the mixture reacted at 1000 °C for 2 h in a NH_4OH–NH_4Cl solution, only the spherical particles of η-Al_2O_3 were detected by SEM as shown in Fig. 7. The ZnK_α and AlK_α profiles on the spots A and B were almost same. From the ratio of the intensity of ZnK_α and AlK_α, it was estimated to be about 35% of the fractional formation (α) of $ZnAl_2O_4$. In the case of the reaction in the ZnO(S)–η-Al_2O_3 mixture, similar phenomena were observed and the fractional formation (α) was estimated to be about 80%.

From the above results, it can be concluded that the product layer of $ZnAl_2O_4$ formed at the surface of η-Al_2O_3 particles, not of ZnO particles, supporting the mechanism of $ZnAl_2O_4$ formation in air described in the previous paper [3]. The mechanism of $ZnAl_2O_4$ formation in air includes the following steps: (a) vapour transport of ZnO to the outer surface of η-Al_2O_3; (b) surface reaction for $ZnAl_2O_4$ formation at the η-Al_2O_3 surface; (c) diffusion of reactants through the $ZnAl_2O_4$ layer, and (d) phase–boundary reaction at the ZnO/$ZnAl_2O_4$ and $ZnAl_2O_4$/η-Al_2O_3 interfaces. In general, the reaction rate of $ZnAl_2O_4$ formation in air obeys the diffusion-controlled Jander's equation [4, 5], which indicates that step (c) is the rate-controlling step.

Moreover, it has been found that the use of monodispersed, uniform particles of ZnO and η-Al_2O_3 was favourable for: (i) obtaining useful information on the reaction mechanism, because of the ease of SEM observation of the change in size and microstructure of reaction particles during the reaction and (ii) forming monodispersed, spherical $ZnAl_2O_4$ particles depending on the morphology of alumina.

References

1. T. TSUCHIDA and S. KITAJIMA, *Chem. Lett.* (1990) 1769.
2. T. TSUCHIDA and H. BETSUYAKU, *Bull. Fac. Eng. Hokkaido Univ.* **149** (1990) 119.
3. T. TSUCHIDA, *J. Amer. Ceram. Soc.* **71** (1988) C-404.
4. T. TSUCHIDA, R. FURUICHI and T. ISHII, *Z. Anorg. Allg. Chem.* **415** (1975) 175.
5. *Idem., ibid.* **423** (1976) 180.

Received 22 January
and accepted 1 May 1991